Applied Mathematics and Computation 307 (2017) 50–61

Contents lists available at ScienceDirect

Applied Mathematics and Computation

journal homepage: www.elsevier.com/locate/amc

Numerical solutions of coupled Klein–Gordon–Zakharov equations by quintic B-spline differential quadrature method

Roshan Thoudam

Department of Mathematics, Sikkim University, 6th Mile, Samdur, Tadong, Gangtok 737102, Sikkim, India

ARTICLE INFO

Keywords:
Conservative quantity
Differential quadrature
Klein–Gordon–Zakharov equations
Quintic B-spline function
Single soliton

ABSTRACT

Numerical solutions of the coupled Klein–Gordon–Zakharov equations are obtained by using quintic B-spline based differential quadrature method. A Runge–Kutta fourth method is used for time integration. Stability of the scheme is studied using matrix stability analysis. The accuracy and efficiency of the presented method is shown by conducting some numerical experiments on test problems which includes the motion of single soliton and interactions of two solitons. The numerical results are found in good agreement with the exact solutions.

1. Introduction

The coupled Klein–Gordon–Zakharov (KGZ) equations were introduced by Dendy [1], to model the interactions between the Langmuir waves and the ion acoustic waves in plasma. Denoting the fast time scale of electric field of the electron by the complex function $U(x, t)$ and the deviation of density from its equilibrium by the real function $N(x, t)$, the one-dimensional KGZ system takes the form:

$$U_{tt} - U_{xx} + U + NU + |U|^2 U = 0, \tag{1}$$

$$N_{tt} - N_{xx} = \left(|U|^2\right)_{xx}, \tag{2}$$

with the initial conditions

$$\left.\begin{aligned} U(x,0) &= U_0(x);\ U_t(x,0) = U_1(x), \\ N(x,0) &= N_0(x);\ N_t(x,0) = N_1(x), \end{aligned}\right\} \tag{3}$$

and the boundary conditions

$$\left.\begin{aligned} U(a,t) &= U_a(t);\ U(b,t) = U_b(t), \\ N(a,t) &= N_a(t);\ N(b,t) = N_b(t), \end{aligned}\right\} \tag{4}$$

where $x \in \Omega = [a, b] \subset R$ and $0 \le t \le T$.

The initial-boundary value problem (1)–(4) possesses the following conservative quantity:

$$E = \int_a^b \left[|U_t|^2 + |U_x|^2 + |U|^2 + N|U|^2 + \frac{1}{2}|V|^2 + \frac{1}{2}|N|^2 + \frac{1}{2}|U|^4 \right] dx = const, \tag{5}$$

where the potential V is define as $V = -f_x,\ f_{xx} = N_t$.

E-mail address: roshandmc@gmail.com

http://dx.doi.org/10.1016/j.amc.2017.02.049
0096-3003/

Well posedness of the KGZ equations has been proved by Ozawa et al. [2] in three space dimensions and the global solutions of the equations has also been obtained by Boling and Guangwei [3–5]. The stability behavior of solitary waves for KGZ equations are discuss in [6,7]. As coupled equations, KGZ equations have a similar shaped to Zakharov and Klein–Gordon–Schrodinger equations. Analytical methods are applied and exact solutions are obtained in [8–10] for KGZ equations. Li [10] obtained the exact explicit travelling wave solutions for $(n+1)$-dimensional KGZ equations. In [8,9] solitons and conoidal waves of the KGZ equations are obtained by applying the solitary wave Ansatz method, the travelling wave hypothesis method, the (G'/G) method and the mapping method. Solitons are solitary waves with an elastic property. They appear as a result of a balance between weak nonlinearity and dispersion. Solitons retain their shapes and speed after colliding with each other. An extensive overview of the soliton solutions of some well-known partial differential equations have been found in [11–20].

A few numerical methods have been proposed for KGZ equations. Multisymplectic numerical methods that preserve the discrete multisymplectic conservative law had studied by Wang [21] for solitary wave propagation and interaction of the KGZ equations. In [22] Wang et al. derived an explicit and an implicit conservative difference schemes for the KGZ equations. A finite difference scheme with a parameter θ has been proposed by Chen and Zhang [23]. Also, Ghoreishi et al. [24] used Chebyshev Cardinal Functions and employing the operational matrices for derivatives, they reduce the PDE to nonlinear algebraic equations. In [25] Dehghan and Nikpour proposed, the differential quadrature and globally radial basis function methods for the numerical solutions of the KGZ equations.

Differential quadrature method (DQM) was first introduced by Bellman et al. [26] in 1972 to solve ordinary and partial differential equations. This method approximates the derivatives of a function at a certain point using weighted sum of the functional values at certain discrete points. Many authors have used various basis functions to develop various types of DQMs. Legendre polynomials, Lagrange interpolation polynomials, spline functions, radial basis functions, etc. are some of them [26–30] that can be counted. One of the best methods was developed by Shu and Rechards using Lagrange interpolation polynomials as test function [31]. They obtained explicit formulations to compute the weighting coefficients. In the recent years, the DQM has been widely popular due to its easy applicability, stability, high accuracy and adaptation with other numerical methods and many engineering/physics problems have been solved successfully using various DQMs [25,32–44].

In this paper, we present a quintic B-spline differential quadrature method (QBS-DQM) to solve the Klein–Gordon–Zakharov equations. We use quintic B-spline basis functions to compute the weighting coefficients. First the KGZ equations are converted into six partial differential equations (PDEs) and then equations are discretized spatially by QBS-DQM. Then we obtained systems of ordinary differential equations (ODEs) in time. The obtained systems of ODEs are solved using RK4 [45] scheme and consequently the approximate solution is obtained. The numerical solutions of a variety of coupled nonlinear PDEs can be obtained by the application of the proposed method without linearization of the original equation and this method can achieved accurate result with less computational time and less number of grid points.

2. Quintic B-spline differential quadrature method (QBS-DQM)

Let us consider the grid distribution $a=x_0 < x_1 < \cdots < x_N=b$ of the finite interval $[a, b]$. Then, based on the differential quadrature theory, the derivative value $u^{(n)}(x)$ with respect to x at a point x_i is given by

$$u^{(n)}(x_i) = \sum_{j=0}^{N} w_{i,j}^{(n)} u(x_j),\ i = 0,\ 1, \ldots,\ N \text{ and } n = 1,\ 2,\ \ldots,\ N-1 \tag{6}$$

where $w_{i,j}^{(n)}$ represents the weighting coefficients, and N is the number of subintervals in which the solution domain $[a, b]$ is divided.

Let $Q_i(x)$ be the quintic B-splines with knots at the point x_i where the uniformly distributed grid points are chosen as $a=x_0 < x_1 < \cdots < x_N=b$ on the ordinary real axis with $h=x_i-x_{i-1}$ $i=1\ldots,N$. The quintic B-spline $Q_i(x)$ at the knots is given by

$$Q_i(x) = \frac{1}{h^5}\begin{cases} (x-x_{i-3})^5 & x \in [x_{i-3}, x_{i-2}) \\ (x-x_{i-3})^5 - 6(x-x_{i-2})^5 & x \in [x_{i-2}, x_{i-1}) \\ (x-x_{i-3})^5 - 6(x-x_{i-2})^5 + 15(x-x_{i-1})^5 & x \in [x_{i-1}, x_i) \\ (x_{i+3}-x)^5 - 6(x_{i+2}-x)^5 + 15(x_{i+1}-x)^5 & x \in [x_i, x_{i+1}) \\ (x_{i+3}-x)^5 - 6(x_{i+2}-x)^5 & x \in [x_{i+1}, x_{i+2}) \\ (x_{i+3}-x)^5 & x \in [x_{i+2}, x_{i+3}) \\ 0, & otherwise \end{cases}$$

The quintic B-splines $\{Q_{-2}, Q_{-1}, Q_0,\ Q_1,\ \ldots, Q_{N-1}, Q_N, Q_{N+1}, Q_{N+2}\}$ form a basis for functions defined over the domain $[a, b]$. Each quintic B-spline covers six elements so that each element is covered by six quintic B-splines. The values of $Q_i(x)$ and its derivative may be tabulated as in Table 1. Using the quintic B-splines as test functions in the fundamental DQM, Eq.

Table 1
Values of the quintic B-spline $Q_j(x)$ and its derivatives at node x_j.

x	x_{i-3}	x_{i-2}	x_{i-1}	x_i	x_{i+1}	x_{i+2}	x_{i+3}
$Q_i(x)$	0	1	26	66	26	1	0
$Q_i'(x)$	0	$5/h$	$50/h$	0	$-50/h$	$-5/h$	0
$Q_i''(x)$	0	$20/h^2$	$40/h^2$	$-120/h^2$	$40/h^2$	$20/h^2$	0
$Q'''_i(x)$	0	$60/h^3$	$-120/h^3$	0	$120/h^3$	$60/h^3$	0
$Q_i^{iv}(x)$	0	$120/h^4$	$-480/h^4$	$720/h^4$	$-480/h^4$	$120/h^4$	0

(6) leads to the equation

$$\frac{\partial^n Q_m(x_i)}{\partial x^n} = \sum_{j=m-2}^{m+2} w_{i,j}^{(n)} Q_m(x_j), i = 0, 1, \ \ldots, \ N, \ m = -2, -1, \ \ldots, \ N+1, N+2. \tag{7}$$

An arbitrary choice of i leads to an algebraic equation system

$$\begin{pmatrix} Q_{-2,-4} & Q_{-2,-3} & Q_{-2,-2} & Q_{-2,-1} & Q_{-2,0} & & & \\ & Q_{-1,-3} & Q_{-1,-2} & Q_{-1,-1} & Q_{-1,0} & Q_{-1,1} & & \\ & \ddots & \ddots & \ddots & \ddots & \ddots & & \\ & & Q_{N+1,N-1} & Q_{N+1,N} & Q_{N+1,N+1} & Q_{N+1,N+2} & Q_{N+1,N+3} & \\ & & & Q_{N+2,N} & Q_{N+2,N+1} & Q_{N+2,N+2} & Q_{N+2,N+3} & Q_{N+2,N+4} \end{pmatrix} \begin{pmatrix} w_{i,-4}^{(n)} \\ w_{i,-3}^{(n)} \\ \vdots \\ w_{i,N+3}^{(n)} \\ w_{i,N+4}^{(n)} \end{pmatrix} = \psi \tag{8}$$

where $Q_{i,j}$ denotes $Q_i(x_j)$ and $\psi = [\frac{\partial^n Q_{-2}(x_i)}{\partial x^n}, \frac{\partial^n Q_{-1}(x_i)}{\partial x^n}, \ \ldots, \frac{\partial^n Q_{N+1}(x_i)}{\partial x^n}, \frac{\partial^n Q_{N+2}(x_i)}{\partial x^n}]^T$. The system (8) consists of $(N+5)$ equations and $(N+9)$ unknowns. In order to be able to solve Eq. (8), it requires four more additional equations. By the addition of the equations

$$\frac{\partial^{n+1} Q_{-2}(x_i)}{\partial x^{n+1}} = \sum_{j=-4}^{0} w_{ij}^{(n)} Q'_{-2}(x_j), \ \frac{\partial^{n+1} Q_{-1}(x_i)}{\partial x^{n+1}} = \sum_{j=-3}^{1} w_{ij}^{(n)} Q'_{-1}(x_j),$$

$$\frac{\partial^{n+1} Q_{N+1}(x_i)}{\partial x^{n+1}} = \sum_{j=N-1}^{N+3} w_{ij}^{(n)} Q'_{N+1}(x_j) \text{ and } \frac{\partial^{n+1} Q_{N+2}(x_i)}{\partial x^{n+1}} = \sum_{j=N}^{N+4} w_{ij}^{(n)} Q'_{N+2}(x_j)$$

to the system (8) and using the values of the quintic B-splines at the grid points and eliminating $w_{i,-4}^{(n)}$, $w_{i,-3}^{(n)}$, $w_{i,N+3}^{(n)}$ and $w_{i,N+4}^{(n)}$ from the system, we obtain an algebraic equation system having penta-diagonal matrix of the form

$$\Phi W = \Psi \tag{9}$$

where

$$\Phi = \begin{pmatrix} 37 & 82 & 21 & & & & & & \\ 8 & 33 & 18 & 1 & & & & & \\ 1 & 26 & 66 & 26 & 1 & & & & \\ & 1 & 26 & 66 & 26 & 1 & & & \\ & & \ddots & \ddots & \ddots & \ddots & \ddots & & \\ & & & 1 & 26 & 66 & 26 & 1 & \\ & & & & 1 & 26 & 66 & 26 & 1 \\ & & & & & 1 & 18 & 33 & 8 \\ & & & & & & 21 & 82 & 37 \end{pmatrix} \text{ and } W = \begin{pmatrix} w_{i,-2}^{(n)} \\ w_{i,-1}^{(n)} \\ \vdots \\ w_{i,j-2}^{(n)} \\ w_{i,j-1}^{(n)} \\ w_{i,j}^{(n)} \\ w_{i,j+1}^{(n)} \\ w_{i,j+2}^{(n)} \\ \vdots \\ w_{i,N+1}^{(n)} \\ w_{i,N+2}^{(n)} \end{pmatrix}.$$

The non-zero entries of the load vector Ψ are given as:

$$\Psi_{-2} = \frac{1}{30}\left(-5Q_{-2}^{(n)}(x_i) + hQ_{-2}^{(n+1)}(x_i) + 40Q_{-1}^{(n)}(x_i) + 8hQ_{-1}^{(n+1)}(x_i)\right),$$
$$\Psi_{-1} = \frac{1}{10}\left(5Q_{-1}^{(n)}(x_i) - hQ_{-1}^{(n+1)}(x_i)\right),$$
$$\Psi_{i-2} = Q_{i-2}^{(n)},\ \Psi_{i-1} = Q_{i-1}^{(n)},\ \Psi_i = Q_i^{(n)},\ \Psi_{i+1} = Q_{i+1}^{(n)},\ \Psi_{i+2} = Q_{i+2}^{(n)},$$
$$\Psi_{N+1} = \frac{1}{10}\left(5Q_{N+1}^{(n)}(x_i) + hQ_{N+1}^{(n+1)}(x_i)\right),$$
$$\Psi_{N+2} = \frac{-1}{30}\left(5Q_{N+2}^{(n)}(x_i) + hQ_{N+2}^{(n+1)}(x_i) - 40Q_{N+1}^{(n)}(x_i) + 8hQ_{N+1}^{(n+1)}(x_i)\right). \tag{10}$$

The equation system (9) is solved by using a variant of Thomas algorithm at each grid point x_i, $i=0,\ 1,\ \ldots,\ N$ and we get all the weight coefficients $w_{i,j}^{(n)}$, for all $i, j=0,\ 1,\ \ldots,\ N$ and $n=1,\ 2,\ \ldots,\ N-1$.

2.1. Computation of weighting coefficients of second order derivative

We have to compute only the weighting coefficients $w_{i,j}^{(2)}$, at each grid point x_i, using Eqs. (9) and (10), as only the second order derivatives for space are present in the KGZ equations. For example, applying the test function Q_m, $m=-2,\ -1,\ \ldots,\ N+2$ at the first grid point x_0 by selecting $i=0$ and $n=2$ in Eq. (10), we get all the entries of the load matrix Ψ as:

$$\begin{aligned}\Psi_{-2} &= \frac{1}{30}\left(-5Q_{-2}^{(2)}(x_0) + hQ_{-2}^{(3)}(x_0) + 40Q_{-1}^{(2)}(x_0) + 8hQ_{-1}^{(3)}(x_0)\right)\\ &= \frac{1}{30}\left(-5\left(\frac{20}{h^2}\right) + h\left(-\frac{60}{h^3}\right) + 40\left(\frac{40}{h^2}\right) + 8h\left(\frac{120}{h^3}\right)\right) = \frac{80}{h^2},\\ \Psi_{-1} &= \frac{1}{10}\left(5Q_{-1}^{(2)}(x_0) - hQ_{-1}^{(3)}(x_0)\right) = \frac{1}{10}\left(5\left(\frac{40}{h^2}\right) - h\left(\frac{120}{h^3}\right)\right) = \frac{8}{h^2},\\ \Psi_0 &= Q_0^{(2)}(x_0) = -\frac{120}{h^2},\ \Psi_1 = Q_1^{(2)}(x_0) = \frac{40}{h^2},\ \Psi_2 = Q_2^{(2)}(x_0) = \frac{20}{h^2},\end{aligned}$$

and all $\Psi_i=0,\ i=3,\ 4,\ \ldots,\ N+2$.

With this load matrix, we can get the weighting coefficients $w_{0,j}^{(2)},\ j=-2,\ -1,\ \ldots,\ N+2$, from the following system:

$$\Phi W_0 = \Psi_{x_0},$$

where

$$W_0 = \left[w_{0,-2}^{(2)},\ w_{0,-1}^{(2)},\ \ldots, w_{0,j-2}^{(2)}, w_{0,j-1}^{(2)}, w_{0,j}^{(2)}, w_{0,j+1}^{(2)},\ w_{0,j+2}^{(2)}, \ldots, w_{0,N+1}^{(2)},\ w_{0,N+2}^{(2)}\right]^T$$

and

$$\Psi_{x_0} = \left[\frac{80}{h^2}, \frac{8}{h^2}, -\frac{120}{h^2},\ \frac{40}{h^2},\ \frac{20}{h^2},\ 0,\ \ldots,\ 0\right]^{\mathrm{T}}.$$

With the same idea, the weighting coefficients $w_{k,j}^{(2)},\ j=-2,,-1,\ \ldots,\ N+2$ at the grid points x_k, $3 \le k \le N-2$ can be obtained from the following system:

$$\Phi W_k = \Psi_{x_k},$$

where

$$W_k = \left[w_{k,-2}^{(2)},\ w_{k,-1}^{(2)},\ \ldots, w_{k,j-2}^{(2)}, w_{k,j-1}^{(2)}, w_{k,j}^{(2)}, w_{k,j+1}^{(2)},\ w_{k,j+2}^{(2)}, \ldots, w_{k,N+1}^{(2)},\ w_{k,N+2}^{(2)}\right]^T$$

and

$$\Psi_{x_k} = \left[0,\ \ldots, 0,\ \frac{20}{h^2}, \frac{40}{h^2}, -\frac{120}{h^2}, \frac{40}{h^2}, \frac{20}{h^2}, 0,\ \ldots, 0\right]^T.$$

For the last grid point x_N, the weight coefficients $w_{N,j}^{(2)},\ j=-2,\ -1,\ \ldots,\ N+2$ can be determined from the following system:

$$\Phi W_N = \Psi_{x_N},$$

where

$$W_N = \left[w_{N,-2}^{(2)},\ w_{N,-1}^{(2)},\ \ldots, w_{N,j-2}^{(2)}, w_{N,j-1}^{(2)}, w_{N,j}^{(2)}, w_{N,j+1}^{(2)},\ w_{N,j+2}^{(2)}, \ldots, w_{N,N+1}^{(2)},\ w_{N,N+2}^{(2)}\right]^T$$

and

$$\Psi_{x_k} = \left[0,\ \ldots, 0,\ \frac{20}{h^2}, \frac{40}{h^2}, -\frac{120}{h^2}, \frac{8}{h^2}, \frac{80}{h^2}\right]^T.$$

3. Implementation of QBS-DQM

In this section we consider the KGZ Eqs. (1) and (2) with initial and boundary conditions (3) and (4). We set $U(x, t)=p(x, t)+i\,q(x, t)$, $u(x, t)=p_t(x, t)$, $v(x, t)=q_t(x, t)$, $N(x, t)=y(x, t)$ and $z(x, t)=y_t(x, t)$, where $p,\ q,\ u,\ v,\ y$ and z are all real functions of x and t. Using the above substitutions, KGZ Eqs. (1) and (2) reduce to the following six partial differential equations (PDEs):

$$\left.\begin{aligned} p_t &= u \\ u_t &= p_{xx} - yp - \left(p^2+q^2\right)p \\ q_t &= v \\ v_t &= q_{xx} - yq - \left(p^2+q^2\right)q \\ y_t &= z \\ z_t &= y_{xx} + \left(p^2+q^2\right)_{xx} \end{aligned}\right\} \tag{11}$$

To solve this system at the collocation points $\{x_0,\ x_1,\ \ldots,\ x_N\}$, with uniform step size $h=x_i-x_{i-1}$, for $i=1,\ 2,\ \ldots,\ N$, we define the following:

$$\boldsymbol{P}(t) = [p_0(t),\ p_1(t),\ \ldots,\ p_N(t)]^T,\ \boldsymbol{Q}(t) = [q_0(t),\ q_1(t),\ \ldots, q_N(t)]^T,$$

$$\boldsymbol{U}(t) = [u_0(t),\ u_1(t),\ \ldots, u_N]^T,\ \boldsymbol{V}(t) = [v_0(t),\ v_1(t),\ \ldots, v_N]^T,$$

$$\boldsymbol{Y}(t) = [y_0(t),\ y_1(t),\ \ldots,\ y_N]^T,\ \boldsymbol{Z}(t) = [z_0(t),\ z_1(t),\ \ldots,\ z_N(t)]^T$$

and

$$\tilde{\boldsymbol{W}} = \begin{pmatrix} w^{(2)}_{0,0} & w^{(2)}_{0,1} & \cdots & w^{(2)}_{0,N} \\ w^{(2)}_{1,0} & w^{(2)}_{1,1} & \cdots & w^{(2)}_{1,N} \\ \vdots & \vdots & \ddots & \vdots \\ w^{(2)}_{N,0} & w^{(2)}_{N,1} & \cdots & w^{(2)}_{N,N} \end{pmatrix}$$

where $p_i(t) = p(x_i, t)$, $q_i(t) = q(x_i, t)$, $u_i(t) = u(x_i, t)$, $v_i(t) = v(x_i, t)$, $y_i(t) = y(x_i, t)$, $z_i(t) = z(x_i, t)$ for all $i = 0,\ 1,\ \ldots,\ N$.

Using these definitions the system (11) reduces to a system of ODEs, which can be written in the following matrix equations:

$$\left.\begin{aligned} \boldsymbol{P}'(t) &= \boldsymbol{U}(t) \\ \boldsymbol{U}'(t) &= \tilde{\boldsymbol{W}}\cdot\boldsymbol{P}(t) - \boldsymbol{Y}(t) * \boldsymbol{P}(t) - (\boldsymbol{P}(t) * \boldsymbol{P}(t) + \boldsymbol{Q}(t) * \boldsymbol{Q}(t)) * \boldsymbol{P}(t) \\ \boldsymbol{Q}'(t) &= \boldsymbol{V}(t) \\ \boldsymbol{V}'(t) &= \tilde{\boldsymbol{W}}\cdot\boldsymbol{Q}(t) - \boldsymbol{Y}(t) * \boldsymbol{Q}(t) - (\boldsymbol{P}(t) * \boldsymbol{P}(t) + \boldsymbol{Q}(t) * \boldsymbol{Q}(t)) * \boldsymbol{Q}(t) \\ \boldsymbol{Y}'(t) &= \boldsymbol{Z}(t) \\ \boldsymbol{Z}'(t) &= \tilde{\boldsymbol{W}}\cdot(\boldsymbol{Y}(t) + \boldsymbol{P}(t) * \boldsymbol{P}(t) + \boldsymbol{Q}(t) * \boldsymbol{Q}(t)) \end{aligned}\right\} \tag{12}$$

where $'\cdot'$ and $'*'$ denote multiplication of two matrices and component by component multiplication of two matrices.

Using the corresponding initial and boundary conditions (3) and (4) we solve the system of ODEs (12) by RK4 scheme [45].

4. Stability analysis

Unlike the classical finite difference and finite element methods, Von Neuman stability analysis cannot be performed in DQM discretized system, instead matrix stability or energy stability have been studied for DQMs in the literatures [46–48]. After linearization of system of ODEs (12), we can rewrite it in the following compact form:

$$\boldsymbol{X}'(t) = \boldsymbol{A}\cdot\boldsymbol{X}(t) \tag{13}$$

(we use homogeneous boundary conditions)

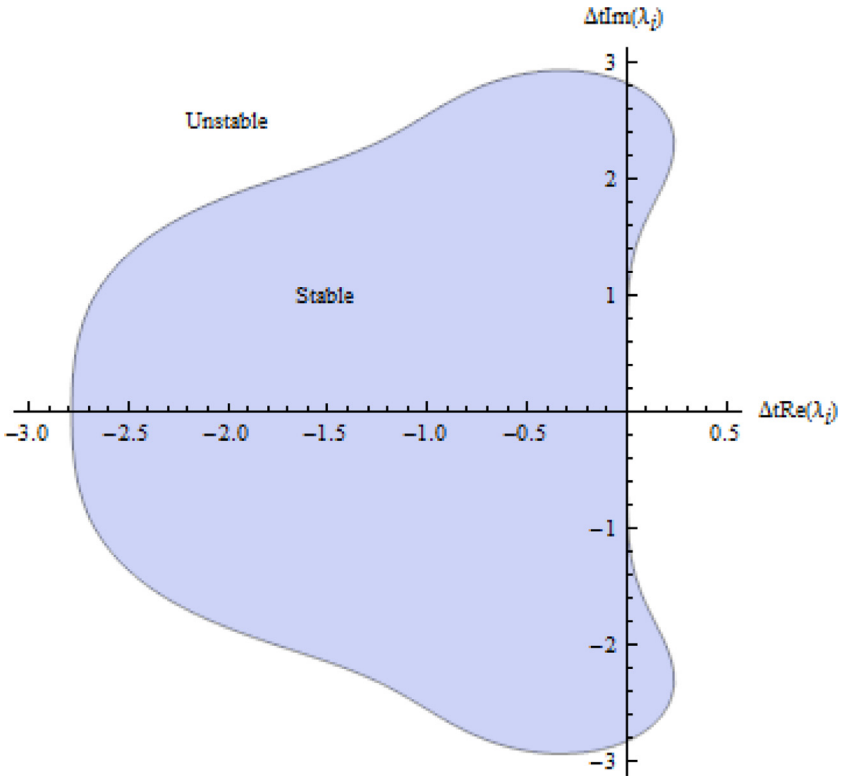

Fig. 1. Stability region for complex eigenvalues.

Or

$$\begin{pmatrix} \boldsymbol{P}'(t) \\ \boldsymbol{U}'(t) \\ \boldsymbol{Q}'(t) \\ \boldsymbol{V}'(t) \\ \boldsymbol{Y}'(t) \\ \boldsymbol{Z}'(t) \end{pmatrix} = \begin{pmatrix} 0 & \boldsymbol{I} & 0 & 0 & 0 & 0 \\ \tilde{\boldsymbol{W}} - \left(\alpha_{p0}^2 + \alpha_{q0}^2\right)\boldsymbol{I} & 0 & 0 & 0 & -\alpha_{p0}\boldsymbol{I} & 0 \\ 0 & 0 & 0 & \boldsymbol{I} & 0 & 0 \\ 0 & 0 & \tilde{\boldsymbol{W}} - \left(\alpha_{p0}^2 + \alpha_{q0}^2\right)\boldsymbol{I} & 0 & -\alpha_{q0}\boldsymbol{I} & 0 \\ 0 & 0 & 0 & 0 & 0 & \boldsymbol{I} \\ 2\alpha_{p0}\tilde{\boldsymbol{W}} & 0 & 2\alpha_{q0}\tilde{\boldsymbol{W}} & 0 & \tilde{\boldsymbol{W}} & 0 \end{pmatrix} \begin{pmatrix} \boldsymbol{P}(t) \\ \boldsymbol{U}(t) \\ \boldsymbol{Q}(t) \\ \boldsymbol{V}(t) \\ \boldsymbol{Y}(t) \\ \boldsymbol{Z}(t) \end{pmatrix}$$

where, 0 and $\boldsymbol{I}$ are zero and identity matrices of order $(N+1)\times(N+1)$ and $\tilde{\boldsymbol{W}}$ is the weighting coefficient matrix for second order derivative approximation as define above. α_{p0} and α_{q0} are absolute maximum norms of the initial vectors $\boldsymbol{P}(0)$ and $\boldsymbol{Q}(0)$ respectively.

The stability of a numerical scheme for numerical integration of Eq. (13) depends on the stability of numerical scheme for solving it. If the system of ODEs (13) is not stable, then the stable numerical scheme for temporal discretization may not generate the converged solution. The stability of Eq. (13) depends on the eigenvalues of coefficient matrix $\boldsymbol{A}$, since its exact solution can be found using the eigenvalues of $\boldsymbol{A}$. Let λ_i be the eigenvalues of the coefficient matrix $\boldsymbol{A}$. The stable solution of $\boldsymbol{X}(t)$ as $t\to\infty$ requires:

(i) if all the eigenvalues are real $-2.78 < \Delta t\lambda_i < 0$
(ii) if eigenvalues have only complex components, $-2\sqrt{2} < \Delta t\lambda_i < 2\sqrt{2}$
(iii) if eigenvalues are complex $\Delta t\lambda_i$ should be in the region shown in Fig. 1.

At the end of Section 5, we will calculate the eigenvalues of the coefficient matrix $\boldsymbol{A}$ and we will see that with the proper choice of Δt, our scheme is stable.

Table 2
L_∞ – errors for $|U|$ and N at different time levels for different time step Δt.

t	$L(\|U\|)_\infty$		$L(N)_\infty$		$CPU-time$		$Conserved-quantity$
	$\Delta t=0.01$	$\Delta t=0.001$	$\Delta t=0.01$	$\Delta t=0.001$	$\Delta t=0.01$	$\Delta t=0.001$	
1	3.53×10^{-5}	3.51×10^{-5}	2.19×10^{-4}	2.20×10^{-4}	0.234	0.954	6.28583
5	9.75×10^{-5}	7.58×10^{-5}	5.65×10^{-4}	3.63×10^{-4}	0.562	4.140	6.28545
8	7.84×10^{-5}	7.90×10^{-5}	4.47×10^{-4}	4.62×10^{-4}	0.797	6.500	6.28573
10	7.82×10^{-5}	8.11×10^{-5}	4.44×10^{-4}	4.55×10^{-4}	0.953	8.063	6.28535

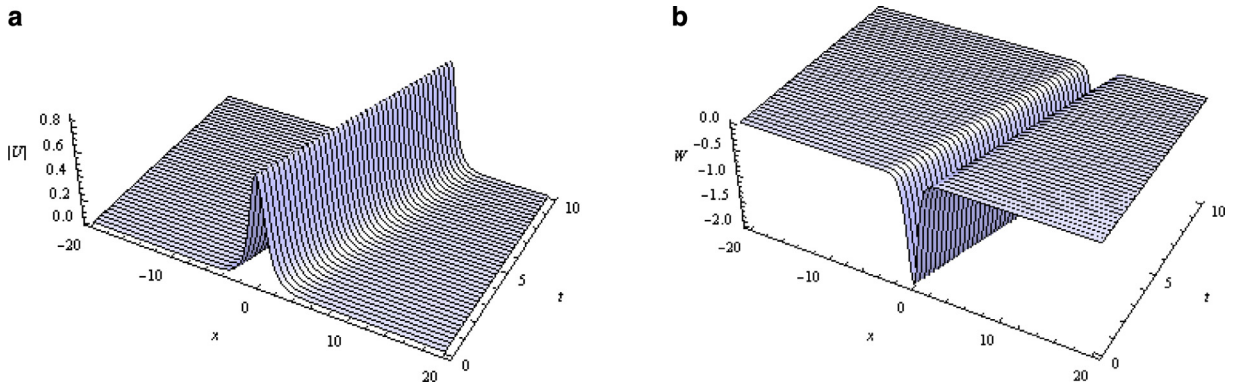

Fig. 2. Space time graph of numerical solution of single soliton for KGZ-equations ($h=0.2$, $\Delta t=0.01$).

5. Numerical experiments

The accuracy and effectiveness of our method is demonstrated in this section. The accuracy of the method is measured using L_∞ error norm which is defined as

$$L_\infty = \underset{0\le i\le N}{Max}\,|u_{exact}(i) - u_{approx}(i)|.$$

The exact solution of the KGZ Eqs. (1) and (2) for single soliton is [9]

$$\begin{aligned} U(x,t,\mu,\vartheta) &= \mu\ sech(\rho(x-\vartheta t))exp(i(-\kappa x+\omega t)),\\ N(x,t,\xi,\vartheta) &= \xi\ sech^2(\rho(x-\vartheta t)), \end{aligned} \tag{14}$$

where μ and ξ are the amplitudes of the U and N solitons respectively. Also ρ and ϑ are the inverse width and velocity of the soliton. Note that $-\kappa x+\omega t$ represent the phase of the soliton where κ and ω represents the soliton frequency and soliton wave number respectively.

The parameters μ, ξ, ρ, ϑ, κ and ω satisfy the following relationship [9]:

$$\mu = \sqrt{\xi\left(\vartheta^2-1\right)},\quad \rho = \pm\sqrt{\frac{\xi+\mu^2}{2\left(\vartheta^2-1\right)}},\quad \omega = \pm\sqrt{\frac{2+\xi+\mu^2}{2\left(\vartheta^2-1\right)}},\quad \kappa = \pm\vartheta\omega. \tag{15}$$

5.1. Motion of a single soliton

With the choice of $\mu=\frac{\sqrt{10}-\sqrt{2}}{2}$, $\vartheta=\sqrt{\frac{\sqrt{5}-1}{2}}$ in (14) and the negative value of ω and positive values for κ and ρ in (15), we obtain [49,50] the exact solutions of KGZ Eqs. (1) and (2) as:

$$\begin{aligned} U(x,t) &= \frac{\sqrt{10}-\sqrt{2}}{2}\ sech\left(\sqrt{\frac{1+\sqrt{5}}{2}}\,x-t\right)\times exp\left(i\left(\sqrt{\frac{2}{1+\sqrt{5}}}\,x-t\right)\right),\\ N(x,t) &= -2\ sech^2\left(\sqrt{\frac{1+\sqrt{5}}{2}}\,x-t\right). \end{aligned} \tag{16}$$

Using the initial and boundary conditions obtained from (16), the KGZ equations is simulated by our method over the solution domain $[-20, 20]$. The L_∞ error for $|U|$ and N in the approximation solution for different time steps $\Delta t=0.01$, 0.001 at different time levels are reported in Table 2. Fig. 2(a)–(b) presents the space-time graph of numerical solution of single soliton up to $t=10$ and Fig. 3(a)–(b) present the error distributions for $|U|$ and N at time $T=10$ when $\Delta t=0.01$. The

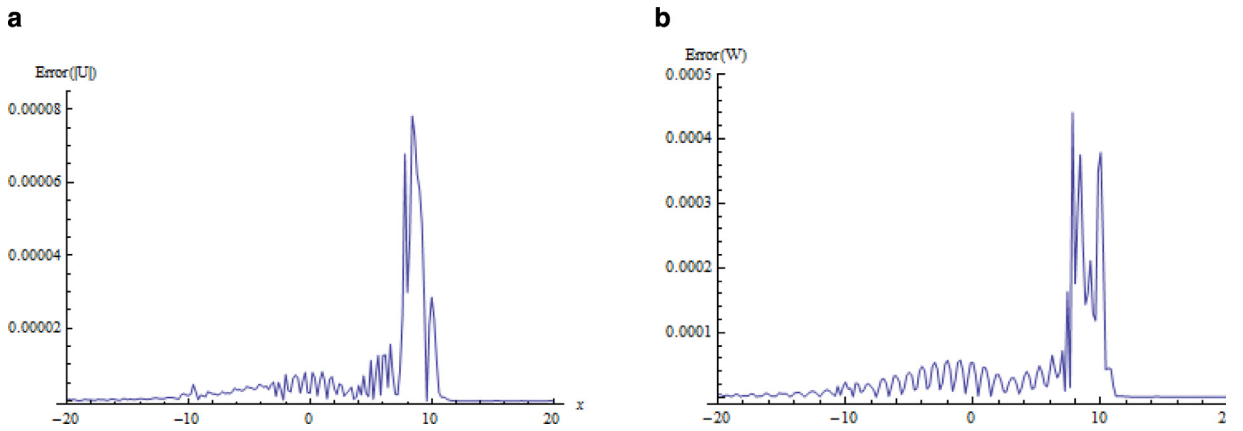

Fig. 3. Error distribution for single soliton solution of KGZ-equations at $t=10$ ($h=0.2$, $\Delta t=0.01$).

Table 3
Comparison of the numerical results with the results found in [25].

Δt	Time, t	Different methods					
		Present	CDQ[25]	IMQ-DQ[25]	TPS-DQ[25]	G-IMQ[25]	G-TPS[25]
	$t=1$						
0.01	$L(\|U\|)_\infty$	3.53×10^{-5}	7.24×10^{-3}	7.24×10^{-3}	7.17×10^{-3}	5.69×10^{-3}	5.69×10^{-3}
	$L(N)_\infty$	3.53×10^{-4}	5.23×10^{-3}	5.29×10^{-3}	7.08×10^{-3}	5.15×10^{-3}	5.00×10^{-3}
0.001	$L(\|U\|)_\infty$	3.51×10^{-5}	0.73×10^{-3}	0.73×10^{-3}	1.05×10^{-3}	0.59×10^{-3}	0.97×10^{-3}
	$L(N)_\infty$	2.20×10^{-4}	0.53×10^{-3}	0.61×10^{-3}	2.99×10^{-3}	0.53×10^{-3}	2.96×10^{-3}
	$t=5$						
0.01	$L(\|U\|)_\infty$	9.75×10^{-5}	3.99×10^{-2}	3.99×10^{-2}	4.07×10^{-2}	3.92×10^{-2}	4.01×10^{-2}
	$L(N)_\infty$	5.65×10^{-4}	4.94×10^{-2}	4.94×10^{-2}	4.99×10^{-2}	4.93×10^{-2}	5.03×10^{-2}
0.001	$L(\|U\|)_\infty$	9.58×10^{-5}	0.41×10^{-2}	0.41×10^{-2}	0.58×10^{-2}	0.40×10^{-2}	0.57×10^{-2}
	$L(N)_\infty$	5.63×10^{-4}	0.52×10^{-2}	0.54×10^{-2}	1.44×10^{-2}	0.53×10^{-2}	1.48×10^{-2}
	$t=10$						
0.01	$L(\|U\|)_\infty$	7.82×10^{-5}	1.10×10^{-1}	1.10×10^{-1}	1.15×10^{-1}	1.10×10^{-1}	1.15×10^{-1}
	$L(N)_\infty$	4.44×10^{-4}	1.16×10^{-1}	1.15×10^{-1}	1.09×10^{-1}	1.14×10^{-1}	1.09×10^{-1}
0.001	$L(\|U\|)_\infty$	8.11×10^{-5}	0.12×10^{-1}	0.12×10^{-1}	0.19×10^{-1}	0.12×10^{-1}	0.19×10^{-1}
	$L(N)_\infty$	4.55×10^{-4}	0.12×10^{-1}	0.12×10^{-1}	0.22×10^{-1}	0.12×10^{-1}	0.22×10^{-1}

Table 4
Comparison of the numerical results with the results found in [9,25].

Method	$T=5$	$2T$	$3T$	$4T$
Present	0.00772	0.01017	0.01098	0.01257
CDQ [25]	0.00798	0.01953	0.03529	0.05580
IMQ-DQ [25]	0.02532	0.03053	0.03676	0.05603
G-IMQ [25]	0.00794	0.01935	0.03531	0.05574
SV-IMQ [25]	0.00798	0.01953	0.03529	0.05580
CH-IMQ [25]	0.00798	0.01953	0.03529	0.05580
[9]	0.00953	0.01091	0.00831	0.01693

numerical results obtained are compared with the results found in [25] and are reported in Table 3. Again for comparison of the present method with the methods presented in [9,25], we consider $\mu=0.5$ and $\vartheta=0.3$ in the interval $[-40, 40]$. The comparison of the L_∞ error between these methods for $|U|$ is shown in Table 4. From Tables 3 to 4, we see that the present method gives more accurate results than the methods found in [9,25] and the computational time is also very less.

We also carry out the numerical convergence studies. For the spatial convergence, we set $\Delta t=0.001$ as the fixed time step and use 5 different spatial meshes: $h=0.8,\ 0.4,\ 0.2,\ 0.1,\ 0.05$, where Δt is sufficiently small such that the temporal error is negligible compare to spatial error. The rate of spatial convergence for the scheme is calculated using the formula: $rate=log(L_\infty(h)/L_\infty(h/2))/log(2)$. The errors and the spatial rate of convergence at $T=5$ are given in Table 5. We see that error decreases when the spatial step size h decreases and the convergence rate increases up to a certain stage and then decreases. Similarly for temporal convergence, we set $h=0.1$ as the fixed space step and $\Delta t=0.1,\ 0.05,\ 0.025,\ 0.0125,\ 0.00625$. The rate of temporal convergence is calculated using similar formula as given above. In Table 6, we present the errors and the

Table 5
Spatial rate of convergence with $\Delta t = 0.001$ at $t = 5$.

h	$L(\|U\|)_\infty$	$rate(\|U\|)$	$L(N)_\infty$	$rate(N)$
0.8	1.0463×10^{-1}		3.8087×10^{-1}	
0.4	7.2467×10^{-3}	3.8518	4.5167×10^{-2}	3.0760
0.2	9.5757×10^{-5}	6.2418	5.1669×10^{-4}	6.3250
0.1	1.2742×10^{-7}	9.5537	6.4587×10^{-6}	6.4467
0.05	5.8287×10^{-8}	1.1283	2.2791×10^{-7}	4.8247

Table 6
Temporal rate of convergence with $h = 0.1$ at $t = 5$.

Δt	$L(\|U\|)_\infty$	$rate(\|U\|)$	$L(N)_\infty$	$rate(N)$
0.1	5.7816×10^{-4}		2.4144×10^{-3}	
0.05	1.4288×10^{-4}	2.0167	5.2443×10^{-4}	2.0094
0.025	3.5636×10^{-5}	2.0034	1.3226×10^{-4}	1.9874
0.0125	8.9671×10^{-6}	1.9906	3.4011×10^{-5}	1.9593
0.00625	2.3144×10^{-6}	1.9540	9.6101×10^{-6}	1.8234

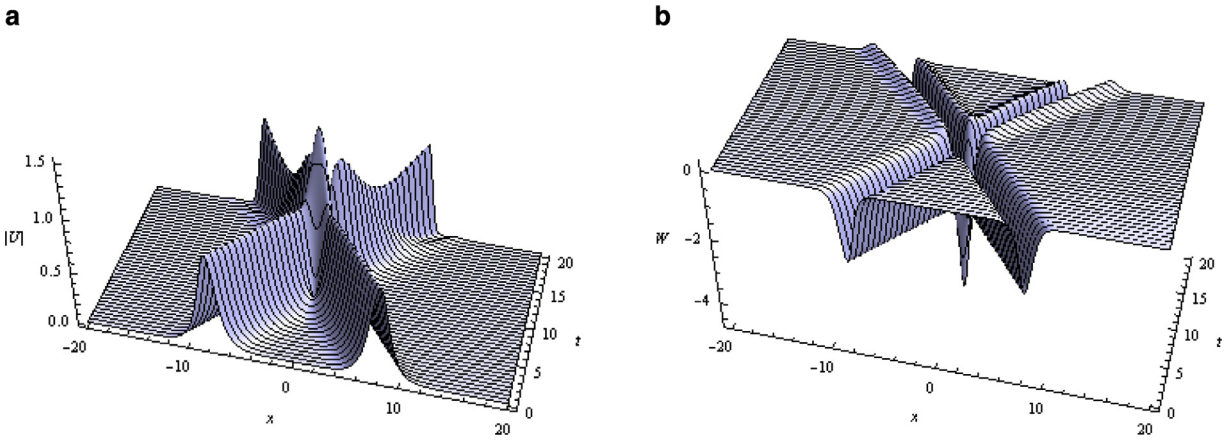

Fig. 4. Space time graph of interaction of two symmetric solitons ($h = 0.2$, $\Delta t = 0.01$).

temporal rate of convergence at $T = 5$. Again, we see that the error decreases when the temporal step size Δt is decrease, and the convergence rate is two.

5.2. Interaction of two solitons

In this example, we consider the interaction of two solitons. The corresponding initial conditions are given as [49]:

$$\begin{aligned} U_0(x) &= U(x - x_1, 0, \mu_1, \vartheta_1) + U(x - x_2, 0, \mu_2, \vartheta_2), \\ U_1(x) &= U_t(x - x_1, t, \mu_1, \vartheta_1)|_{t=0} + U_t(x - x_2, t, \mu_2, \vartheta_2)|_{t=0}, \\ N_0(x) &= N(x - x_1, 0, \xi_1, \vartheta_1) + N(x - x_2, 0, \xi_2, \vartheta_2), \\ N_1(x) &= N_t(x - x_1, t, \xi_1, \vartheta_1)|_{t=0} + N_t(x - x_2, t, \xi_2, \vartheta_2)|_{t=0}. \end{aligned} \tag{17}$$

5.2.1. Interaction of two symmetric solitons

Here we consider the interaction of two solitons with equal amplitudes and opposite velocities. We choose the parameter values $x_1 = -8$, $x_2 = 8$, $\mu_1 = \mu_2 = \frac{\sqrt{10}-\sqrt{2}}{2}$ and $\vartheta_1 = -\vartheta_2 = \sqrt{\frac{\sqrt{5}-1}{2}}$ in the above initial conditions (17) and perform the numerical simulation with the presented method over the solution domain $[-20, 20]$ with time step size $\Delta t = 0.01$ and space step size $h = 0.2$ over the time interval $[0, 20]$. Fig. 4(a)–(b) presents the space-time graph of this interaction by the presented method. In Table 7, the values of the conservative quantity at different time levels and the corresponding CPU time are reported. It can be seen that the present method conserve the conservative quantity, E given in Eq. (4) by almost two decimal places. From Fig. 4, we see that the interaction takes place at about time $T = 10$ and the two solitons completely passes each other at about time $T = 20$. It is clear from the figure that after collision the soliton waves do not preserve themselves. It is found that before collision of the soliton waves, the waveforms keep their amplitudes almost equal. However, after collision, the amplitudes of the two solitons oscillate.

Table 7
The values of the conservative quantity, E and CPU time for interaction of two symmetric solitons at different time levels.

Time, T	$T=0$	$T=5$	$2T$	$3T$	$4T$
Conservative Quantity, E	12.5691	12.5715	12.5722	12.5647	12.5687
CPU-time	0.000	0.657	1.047	1.437	1.843

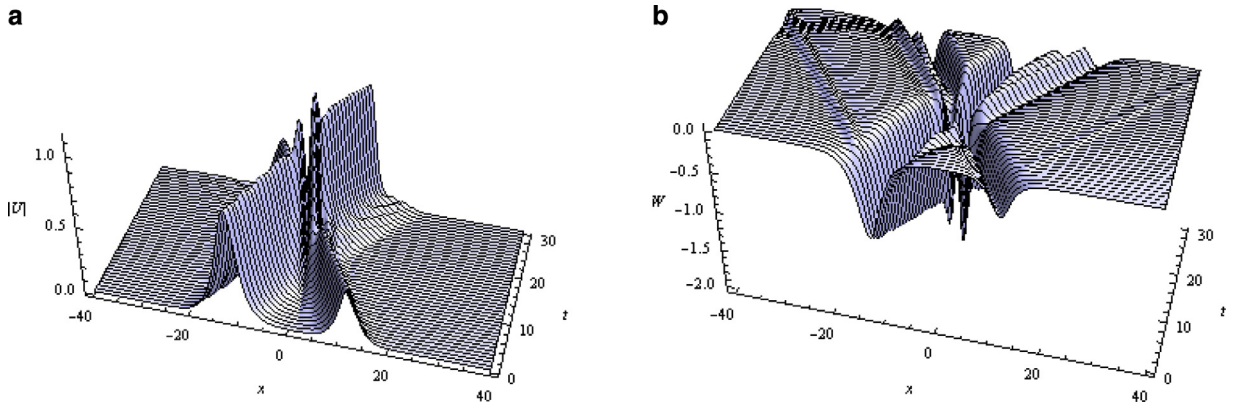

Fig. 5. Space time graph of interaction of two non-symmetric solitons ($h=0.2$, $\Delta t=0.0005$).

Table 8
The values of the conservative quantity, E and CPU time for interaction of two non-symmetric solitons at different time levels.

	$T=0$	$T=5$	$2T$	$3T$	$4T$	$5T$	$6T$
Conservative Quantity, E	11.2475	11.2464	11.3730	11.2623	11.2386	11.2303	11.3840
CPU-time	00.000	11.891	23.797	35.625	48.812	62.016	77.171

5.2.2. Interaction of two non-symmetric solitons

In this case, we choose the following parameter values $x_1=-12$, $x_2=12$, $\mu_1=0.8$, $\mu_2=0.4$, $\vartheta_1=0.6$ and $\vartheta_2=-0.8$ in the initial conditions (17) and perform the simulation with our method over the time interval [0, 30], in the solution domain $[-40, 40]$ with space step $h=0.2$ and time step $\Delta t=0.0005$. Fig. 5(a)–(b) shows the space-time graphs of this interaction of solitons. Form the figure we observed that the larger soliton located at $x=-12$, moved to the right and interacts with a smaller soliton located at $x=12$, which moves to the left at about time $T=10$ and passes completely at about time $T=30$. Table 8 reports the values of the conservative quantity at different time levels and corresponding CPU time. It is seen from the table that the maximum change of the conservative quantity, E from the initial condition is 0.1255 and it takes place when $T=10$, i.e. when the two solitons collide. From the space time graph we also see that after collision the amplitudes of the two solitons oscillate more rapidly than the previous case of symmetric collision.

We calculate the eigenvalues of the coefficient matrix $\boldsymbol{A}$, as defined in (13). We find that $\alpha_{p0}=0.874032$, $\alpha_{q0}=0.328748$ respectively for single soliton and symmetric soliton collision experiments when $N=200$. The maximum of the absolute values of the eigenvalues of the coefficient matrix is found to be 10.9939. The distributions of the eigenvalues in both cases are shown in Fig. 6(a). For the collision of non-symmetric soliton experiment we find that $\alpha_{p0}=0.8$, $\alpha_{q0}=0.512296$ respectively when $N=400$ and the maximum of the absolute values of the eigenvalues of the coefficient matrix is found to be 10.9187. The eigenvalues distribution for this experiment is shown in Fig. 6(b). The information about the eigenvalues gives the idea about the selection of the time step Δt to provide the stability of the method. It is evident that the choice of different time step sizes in our numerical experiments can give stable solutions.

6. Conclusion

In this study, we have constructed quintic B-spline based differential quadrature method for the numerical solutions of the KGZ equations. The weighting coefficients of the derivative approximations are determined by solving a penta-diagonal system of linear equations at each grid points. The KGZ equations are discretized in space by using differential quadrature method approximation and then it reduces to a system of ordinary differential equation in time t. The reduced system of ordinary differential equations is then solved by Pike and Roe's fourth stage RK4 scheme. The accuracy and effectiveness of the presented method is verified by simulating the single soliton motion and the interactions of two solitons. The numerical

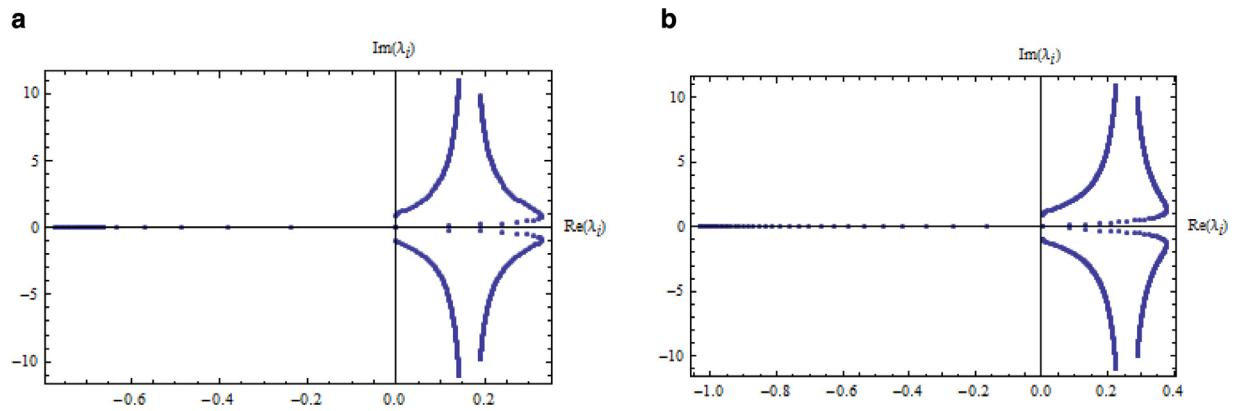

Fig. 6. (a): Distribution of eigenvalues, when $N=200$. (b): Distribution of eigenvalues, when $N=400$.

results show that in comparison with other methods, a very accurate result can be achieve in less computational time, with less number of grid points and larger time step.

Acknowledgment

The author is very thankful to the reviewers for their valuable comments and suggestions to improve the quality of the paper.

This work is supported by the University Grants Commission (UGC), the Government of India, under the scheme UGC-BRS Research Start-Up-Grant (No. F. 30-95/2015(BRS)).

References

[1] R.O. Dendy, Plasma Dynamics, Oxford University Press, Oxford, UK, 1990.
[2] T. Ozawa, K. Tsutaya, Y. Tsutsumi, Well posedness in nergy space for the Cauchy problem of the Klein–Gordon–Zakharov equation with different propagation speeds in three space dimensions, Math. Ann. 313 (1) (1999) 127–140.
[3] G. Boling, Y. Guangwei, Global smooth solution for the Klein–Gordon–Zakharov equations, J. Math. Phys. 36 (1995) 4119–4124.
[4] K. Tsutaya, Global existence of small amplitude solutions of the Klein–Gordon–Zakharov equations, Nonlinear Anal 27 (12) (1996) 1373–1380.
[5] G. Adomain, Non-perturbation solution of Klein–Gordon–Zakharov equations, Appl. Math. Comput. 81 (1997) 89–92.
[6] C. Lin, Orbital stability of solitary waves for the Klein–Gordon–Zakharov equations, Acta Math. Appl. Sin. 15 (1999) 54–64.
[7] J. Zhang, Z. Gan, B. Guo, Stability of the standing waves for a class of coupled nonlinear Klein–Gordon equations, Acta Math. Appl. Sin. 26 (2010) 427–442.
[8] G. Ebadi, E.V. Krishnan, A. Biswas, Solitons and conoidal waves of the Klein–Gordon–Zakharov equation in plasma, Pramana-J. Phys. 79 (2012) 185–198.
[9] M.S. Ismail, A. Biswas, 1-Soliton solution of the Klein–Gordon–Zakharov equation with power law nonlinearity, Appl. Math. Comput. 217 (2010) 4186–4196.
[10] J. Li, Exact explicit travelling wave solutions for $(n+1)$ dimensional Klein–Gordon–Zakharov equations, Chaos Solitons Fract. 34 (2007) 867–871.
[11] Ryan Sassaman, Alireza Heidari, Anjan Biswas, Topological and non-topological solitons of nonlinear Klein–Gordon equations by He's semi-inverse variational principle, J. Frankl. Inst. 347 (7) (2010) 1148–1157.
[12] Anjan Biswas, Daniela Milovic, Arjuna Ranasinghe, Solitary waves of Boussinesq equation in power law media, Commun. Nonlinear Sci. Numer. Simul. 14 (11) (2009) 3738–3742.
[13] Anjan Biswas, Dispersion-managed solitons in optical fibres, J. Opt. A: Pure Appl. Opt. 4 (1) (2002) 84–97.
[14] Michelle Savescu, A.H. Bhrawy, A.A. Alshaery, E.M. Hilal, Kaisar R. Khan, M.F. Mahmood, Anjan Biswas, Optical solitons in nonlinear directional couplers with spatio-temporal dispersion, J. Modern Opt. 61 (5) (2014) 442–459.
[15] Ghodrat Ebadi, A.H. Kara, Marko D. Petkovic, Ahmet Yildirim, Anjan Biswas, Solitons and conserved quantities of the ITO equation, Proc. Roman. Acad., Ser. A 13 (3) (2012) 215–224.
[16] Yanan Xu, Michelle Savescu, Kaisar R. Khan, Mohammad F. Mahmood, Anjan Biswas, Milivoj Belic, Soliton propagation through nano-scale waveguides in optical metamaterials, Opt. Laser Technol. 77 (2016) 177–186.
[17] M. Mirzazadeh, Mostafa Eslami, Michelle Savescu, A.H. Bhrawy, A.A. Alshaery, E.M. Hilal, Anjan Biswas, Optical solitons in DWDM system with spatio-temporal dispersion, J. Nonlinear Opt. Phys. Mater. 24 (1) (2015) 1550006 (28 pages).
[18] Yanan Xu, Qin Zhou, A.H. Bhrawy, Kaisar R. Khan, M.F. Mahmood, Anjan Biswas, Milivoj Belic, Bright solitons in optical metamaterials by travelling wave hypothesis, Optoelectron. Adv. Mater. – Rapid Commun. 9 (2015) 384–387.
[19] M. Savescu, A.A. Alshaery, E.M. Hilal, A.H. Bhrway, Qin Zhou, A. Biswas, Optical solitons in DWDM system with four-wave mixing, Optoelectron. Adv. Mater. – Rapid Commun. 9 (1-2) (2015) 14–19.
[20] M. Eslami, B. Fathi Vajargah, M. Mirzazadeh, A. Biswas, Application of first integral method to fractional partial differential equations, Indian J. Phys. 88 (2) (2014) 177–184.
[21] J. Wang, Solitary wave propagation and interactions for the Klein–Gordon–Zakharov equations in plasma physics, J. Phys. A: Math. Theor. 42 (2009) 085205 (17 pages).
[22] T. Wang, J. Chen, L. Zhang, Conservative difference methods for the Klein–Gordon–Zakharov equations, J. Comput. Appl. Math. 205 (2007) 430–452.
[23] J. Chen, L. Zhang, Numerical simulation for the initial-boundary value problem of the Klein–Gordon–Zakharov equations, Acta Math. Appl. Sin. 28 (2012) 325–336.
[24] M. Ghoreishi, A.I.B.Md. Ismail, A. Rashidy, Numerical solution of Klein–Gordon–Zakharov equations using Chebyshev cardinal functions, J. Comput. Anal. Appl. 14 (2012) 574–582.
[25] M. Dehghan, A. Nikpour, The solitary wave solution of the coupled Klein–Gordon–Zakharov equations via two different numerical methods, Comput. Phys. Commun. 184 (2013) 2145–2158.

[26] R. Bellman, B.G. Kashef, J. Casti, Differential quadrature: a technique for the rapid solution of nonlinear differential equations, J. Comput. Phys. 10 (1972) 40–52.
[27] R. Bellman, B.G. Kashef, E.S. Lee, R. Vasudevan, Differential quadrature and splines, Comput. Math. Appl. 1 (1975) 371–376.
[28] C. Shu, Y.L. Wu, Integrated radial basis function-based differential quadrature method and its performance, Int. J. Numer. Methods Fluids 53 (2007) 969–987.
[29] J.R. Quan, C.T. Chang, New insights in solving distributed system equations by the quadrature methods-I, Comput. Chem. Eng. 13 (1989) 779–788.
[30] J.R. Quan, C.T. Chang, New insights in solving distributed system equations by the quadrature methods-II, Comput. Chem. Eng. 13 (1989) 1017–1024.
[31] C. Shu, B.E. Rechards, Applications of generalized differential quadrature to solve two-dimensional incompressible Navier–Stokes equations, Int. J. Numer. Methods Fluids 13 (1992) 791–798.
[32] A. Korkmaz, I. Dag, A differential quadrature algorithm for simulation of nonlinear Schrödinger equation, Comput. Math. Appl. 59 (2008) 2222–2234.
[33] B. Saka, I. Dag, Y. Dereli, A Korkmaz, Three different methods for numerical solutions of EW equation, Eng. Anal. Bound. Elements 32 (2008) 556–566.
[34] A. Korkmaz, I. Dag, A differential quadrature algorithm for nonlinear schrodinger equation, Nonlinear Dyn. 56 (2009) 1–2.
[35] A. Korkmaz, I. Dag, Crank–Nicolson differential quadrature algorithms for the Kawahara equation, Chaos Soitons Fract. 42 (1) (2009) 65–73.
[36] A. Korkmaz, I. Dag, Solitary wave simulations of complex modified kortweg-de vries equation using differential quadrature method, Comput. Phys. Commun. 180 (9) (2009) 1516–1523.
[37] I. Dag, A. Korkmaz, B. Saka, Cosine expansion based differential quadrature algorithm for numerical solution of the RLW equation, Numer. Methods Partial Differ. Equ. 26 (3) (2010) 544–560.
[38] A. Korkmaz, Numerical algorithms for solutions of Kortweg-de Vries equation, Numer. Methods Partial Differ. Equ. 26 (6) (2010) 1504–1521.
[39] A. Korkmaz, I. Dag, Numerical simulations of complex modified KdV equation using polynomial differential quadrature method, J. Math. Stat. 10 (11) (2011) 1–13.
[40] A. Korkmaz, I. Dag, Cubic B-spline differential quadrature methods for the advection–diffusion equation, Int. J. Numer. Methods Heat Fluid Flow 22 (2012) 1021–1036.
[41] A. Korkmaz, A.M. Aksoy, I. Dag, Quartic B-spline differential quadrature method, Int. J. Nonlinear Sci. 11 (4) (2011) 403–411.
[42] R.C. Mittal, R. Jiwari, Differential quadrature method for two dimensional Burgers' equations, Int. J. Comput. Methods Eng. Sci. Mech. 10 (2009) 450–459.
[43] R. Jiwari, S. Pandit, R.C. Mittal, Numerical simulation of two-dimensional sine-Gordon solitons by differential quadrature method, Comput. Phys. Commun. 183 (2012) 600–616.
[44] R.C. Mittal, R. Bhatia, A numerical study of two dimensional hyperbolic telegraph equation by modified B-spline differential quadrature method, Appl. Math. Comput. 244 (2014) 976–997.
[45] J. Pike, PL. Roe, Accelerated convergence of Jameson's finite volume Euler scheme using Van Der Houwen Integrators, Comput. Fluids 13 (1985) 223–236.
[46] S. Tomasiello, Stability and accuracy of the iterative differential quadrature method, Int. J. Numer. Methods Eng. 58 (6) (2003) 1277–1296.
[47] S. Tomasiello, numerical stability of DQ solutions of wave problems, Numer. Algorithms 57 (3) (2011) 289–312.
[48] S. Tomasiello, Stability and accuracy of DQ-based step-by-step integration methods for structural dynamics, Appl. Math. Model. 37 (5) (2013) 3426–3435.
[49] S.K. Liu, Z.T. Fu, The periodic solutions for a class of coupled nonlinear Klein–Gordon equations, Phys. Lett. A 323 (2004) 415–420.
[50] S.K. Liu, Z.T. Fu, Jacobi elliptic function expansion method and periodic wave solutions of nonlinear wave equations, Phys. Lett. A 289 (2001) 69–74.